Materials Chemistry and Physics 307 (2023) 128194

Contents lists available at ScienceDirect

Materials Chemistry and Physics

journal homepage: www.elsevier.com/locate/matchemphys

Evaluation of acrylic and silane coatings on limestone through macroscopic and microscopic analyses

Francesco Gabriele, Cinzia Casieri, Alice Vetrano, Nicoletta Spreti *

Department of Physical and Chemical Sciences, University of L'Aquila, Coppito, I-67100, L'Aquila, Italy

HIGHLIGHTS

- The performance of silane and acrylic coatings in protecting artworks was evaluated.
- The effect of the coatings on surface hydrophobicity and chromaticity was studied.
- NMR provided water absorption kinetics and pore size distribution of the stone.
- SEM-EDS and micro-FTIR were used to analyze the distribution of the products.
- Our results could be very useful for choosing the most suitable protective product.

GRAPHICAL ABSTRACT

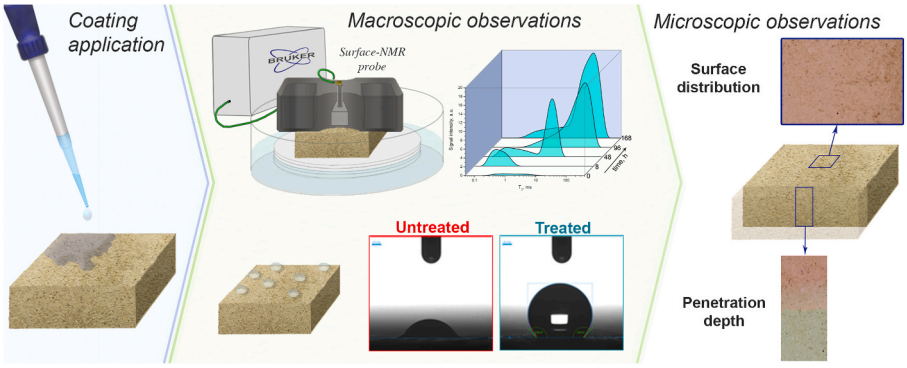

ARTICLE INFO

Keywords:
Acrylic coating
Silane-based coating
Limestone
Hydrophobicity
Water-uptake
Stone protection
Water penetration

ABSTRACT

The aim of this study was to obtain useful information about the behavior of a coating when it interacts with a stone substrate, to allow the choice of the most suitable protective agent to preserve stone artworks from deterioration phenomena in their environmental conditions. The effect of some commercially available silane-based polymers on Lecce stone was compared with that of two new acrylic ones not yet available for sale. The performance of each protective treatment was evaluated by colorimetry, contact angle measurements and NMR relaxometry, which allows to estimate the hygroscopic properties of the stone in terms of open porosity and water-uptake. The microscopic observations combined with micro-FTIR and SEM-EDS analyses were performed to investigate the distribution of the protectives on the stone surface and their depth of penetration. The results showed that the water repellency of the two acrylic products and of one of the silane-based protectives was mainly due to a surface effect, just slowing down water adsorption. On the contrary, the other two silane-based products turned out distributed throughout most of the sample volume, completely hindering water absorption.

1. Introduction

Most of the artistic monumental heritage has stone as support material that is subjected to chemical and physical decay, almost always linked to the suffered environmental conditions. An appropriate strategy, aimed at the preservation of stone works of art, is needed and has to

* Corresponding author.
E-mail address: nicoletta.spreti@univaq.it (N. Spreti).

https://doi.org/10.1016/j.matchemphys.2023.128194
Received 25 May 2023; Received in revised form 3 July 2023; Accepted 15 July 2023
Available online 17 July 2023

be started from a deep knowledge of the stone material, of the products that are called to the conservation and of their mutual interaction. The stone deterioration depends on extrinsic factors such as humidity, temperature, chemical and biological pollutants, and on the intrinsic stone characteristics, such as mineralogical composition, texture and porous structure [1,2]. Various weathering processes may take place within a porous inorganic substrate in presence of water and deliquescent salts.

Water plays an important role in the decay process of stones; it can easily penetrate into the porous structure, damaging the material through freezing-thawing or wetting-drying cycles. Furthermore, it can transport soluble salts, which penetrate the stone and crystallize, inducing both the formation of efflorescence and mechanical stress and thus determining a limited durability over time. In general, large damage effects may be observed in porous materials with high open porosity and well-interconnected pores, as water-assisted migration, entrapment, and partial dissolution of pollutants within inner regions of the porous medium are favored.

Water is also responsible for the formation of biological patinas and, in an environment with high levels of humidity and exposure to light, microorganisms can proliferate on stone surfaces, causing the biodegradation of the stone [3–5].

Further structural damages can occur mainly either due to a thermal stress, *i.e.,* when different surface portions of the same artifact are simultaneously affected by different temperatures, or when they are constituted of heterogeneous materials with different thermal expansion coefficients.

In order to preserve the stone artworks, it is necessary to apply a protective barrier between the stone and the external agents, in particular water. For this purpose, it is necessary to reduce the wettability of the material without altering its original permeability to water vapor, allowing the rebalancing of the stone moisture content according to environmental conditions. Coatings have to penetrate inside the porous materials by covering their pores, but avoiding the formation of thin layer deposited on their surfaces that could hinder the natural exchanges of water vapor between stone and environment [6].

Since ancient times, natural hydrophobic compounds, such as oils, resins and waxes, are used as water repellents for the protection of stone surfaces [7], but continuously new natural and synthetic polymeric materials are proposed as protective and water-repellent products for stone artworks. In accordance with the current European Standard [8], they should possess some requirements when they are applied to stone: the reduction of liquid water absorption with a minimum change of the substrate permeability to water vapor, the maintaining of the original color and gloss of the substrate and of its physical and chemical properties. Moreover, they should not produce by-products that could be harmful to humans and the environment.

Recent papers review the results obtained by comparing products, materials and treatment procedures [9–16]. Acrylic and silicon-based polymers, perfluoropolyethers and fluorinated polymers are the most commonly used products as hydrophobic coatings. Acrylic resins, such as Paraloid B72, an ethyl methacrylate-methylacrylate copolymer, have been employed for a long time as protective and consolidant coatings for outdoor stone artworks [17,18]. However, its sensitivity to photo-oxidative aging leads to the formation of cross-linked structures with the consequent decrease in product removability and in waterproofing behavior [19]. Fluorinated acrylic copolymers [20–23] or water-based silica/acrylates hybrid coatings [24,25] were developed to overcome these drawbacks and to improve the efficacy of acrylic-based products. The silane-based compounds confer both superhydrophobic and superoleophobic properties to the surfaces [26]. They have been widely used in stone protection since they possess high chemical stability, resistance to UV and thermo-oxidation, and good elasticity [27]. However, they are more effective on siliceous stones than carbonate ones, as they can generate chemical bonds. Anyway, several laboratory studies have been performed to evaluate the performance of silane-based protective agents on carbonate substrates and, in most cases, they were able to confer high hydrophobicity to the treated surface and a slowdown in water adsorption, without significantly altering the chromaticity of the substrate [28,29].

Our previous studies on the protective properties of some widely used commercial products on different limestones revealed that, in lithotypes with higher pore dimensions, some protectives obstructed the surface porosity of the stone samples, preventing their necessary moisture equilibrium and causing in some cases, as for Paraloid B72, a high darkening and yellowing of the treated surfaces [30]. Other studies in the literature proved that the use of commercially available acrylic resins does not fulfill many conservation requirements and therefore should be avoided [18].

The research presented here is part of the Smart City project, focused on "Product and process innovation for the maintenance, conservation and sustainable restoration of cultural heritage". Since case studies were foreseen in the UNESCO site "Sassi and the Rupestrian Churches of Matera", our activity was focused on the comparative evaluation of protective and/or consolidating products for calcarenite stones. In fact, before any treatment on a case study, it is necessary to evaluate its effect on a model support with the final goal to obtain information that could be useful to choose the most suitable protective product, also according to the specific environmental conditions suffered by the artifact under intervention.

In the here presented work, five protective coatings were compared, three of which silane/siloxane-based, which were the most employed class of protectives in cultural heritage field [31,32], and two new acrylics, synthesized by Icap Leather Chem S.p.A. (Milan, Italy), not yet available for sale. Acrylic polymers are generally known as good hydrophobic materials but, as aforementioned, they were no longer applied mainly due to their negative side effects of the treated surfaces.

Protectives were applied on Lecce stone specimens, one of the main building materials in historical Baroque monuments in southern Italy. In particular, the effects of these products on the samples were assessed in terms of (*i*) surface hydrophobicity and chromaticity (*ii*) hygroscopic behavior during water uptake, (*iii*) porosity, (*iv*) distribution of the products on the stone surface and (*v*) their penetration depth into the stone volume.

In particular, NMR relaxometry was used as a non-destructive and non-invasive technique to evaluate the effect of treatment on both the open porosity and the diffusion of water inside the structure with respect to the untreated one [33–36]. Micro-FTIR or SEM-EDS analyses, according to the nature of the protective material, were performed as a very effective method to analyze point by point the coating distribution [37,38].

2. Experimental section

2.1. Materials

Lecce stone (LS) is a fine-grained calcarenite stone, composed of 93–97% calcium carbonate and with a characteristic pale-yellow color. The porosity is around 31–45%, with two Gaussian pore size distribution centered at 0.1 ÷ 0.2 μm and 0.5 ÷ 4 μm [39–41]. LS samples of approximately $5 \times 5 \times 2\ cm^3$ were purchased from DÉCOR, (Monteroni, Italy).

The commercial coatings chosen for the experimentation were: ETS WR® (WR), a water-repellent tetraethyl orthosilicate-based consolidator in isopropyl alcohol by Mapei S.p.A. (Milan, Italy); Hydrophase® Acqua (HY), a water dispersed alkyl/alkoxysilanic resin with catalyst by Phase Restauro S.r.l., (Florence, Italy) and Nanoprotect (NP), an alkyl polysiloxane-based material in water by I.M.A.R. Italia S.p.A. (Rome, Italy). We also focused our attention on two newly synthesized water-based polyacrylic polymer coatings, Polyrest HR2 (HR2) and Polyrest HR3 (HR3), produced and kindly provided to us by ICAP Leather Chem S.p.A. (Milan, Italy).

2.2. Coating procedure

Three LS specimens of similar mass (~80 g) were selected for each treatment; before applying the protective products, the samples were dried in an oven at 60 °C, until they reached the dry weight.

The WR, HY and NP as provided by the producers, and HR2 and HR3 as water dispersions (10%), were homogeneously distributed on one of the stone surfaces (25 cm^2) using a graduated pipette until surface saturation, to accurately control the amount of protective added to the specimens. The solvents were allowed to evaporate in air for eight weeks and then the stone specimens were dried in an oven at 60 °C to determine the dry residues, Q. It was determined according to the following equation:

$$Q = \frac{(m_A - m_B)}{m_B} \times 1000 \quad (1)$$

where m_B and m_A are the stone dry masses, before and after the treatment.

2.3. Static contact angle

The wettability of the stone surface was monitored by the measurement of the static contact angle, using a Krüss Drop Shape Analyzer DSA100 instrument. For each measurement, a deionized water droplet (5 μL) was deposited on the sample surface at room temperature. The drop profile was extrapolated using an appropriate fitting function, and, considering the natural inhomogeneity of the stone material, the mean contact angle of a surface was achieved by averaging on nine measurements performed on different points of the surface.

2.4. Colorimetry

Chromatic changes of stone surfaces induced by the protective coatings were evaluated by colorimetric analysis performed before and after polymer applications by means of Sama Tools SA230 portable colorimeter. Measurements were performed in SCE mode with an 8° standard observer, light D65 (average daylight, including the UV region, with the relative color temperature of 6504 K) and 25 points *per* sample were taken with the aid of a 5 × 5 grid to cover an overall surface of 60%. Colorimetric values were determined by using the CIELAB color space proposed in 1976 by the International Lighting Commission (CIE) [42]. Results were elaborated on the basis of the chromatic coordinates in CIE-L*a*b* standard color system. When compared to a reference, the color alterations suffered by a sample were evaluated by the difference ΔE*, expressed as:

$$\Delta E^* = \sqrt{\Delta L^{*2} + \Delta a^{*2} + \Delta b^{*2}} \quad (2)$$

where ΔL*, Δa* and Δb* represent the difference of each chromatic coordinate between the measured sample and the reference.

2.5. Hygroscopic properties and porosity

The NMR equipment mq-ProFiler (Bruker, Italy), consisting of a surface probe and a portable electronic apparatus, was used to study the hygroscopic behavior and the porosity of the samples thorough NMR porosimetry, *i.e.*, transverse relaxation time (T_2) measurements [33]. The NMR signals were acquired using the CPMG with the shortest echo-time $2\tau = 44$ μs to reduce the diffusion effect. For every measurement of T_2 it was necessary to acquire 3000 echoes to cover the entire relaxation curves. Moreover, each sequence was repeated every 2 s for 512 times to maximize the signal-to-noise ratio, within a reasonable measurement time (~15 min). The coil in use works at a Larmor frequency of 17.8 MHz, which can excite the sample up to a depth of about 2 mm and with a sensitive volume (x, y, z) of about 2 × 0.2 × 0.8 cm^3.

The water absorption tests were carried out by capillarity, during water uptake, both on reference and treated samples. In particular, the stone samples were dried in an oven at 60 °C until they reached the dry condition and placed on filter paper (thickness 1 cm and diameter 9 cm) constantly saturated with water, according to the European Standard [43]. While the face in contact with the water was the treated one, the other face was put in contact with the NMR surface probe. The NMR signals acquired at fixed times during the capillary absorption, were processed using the inverse Laplace transform with the UPEN algorithm (UpenWin, villiam.bortolotti@unibo.it), to obtain the T_2-distributions during the kinetics of water absorption. The extrapolated equilibrium magnetization, obtained by UPEN in arbitrary units, allowed estimating the material's water content in the sensitive volume of the NMR surface probe [44].

Open porosity of reference and treated samples was evaluated by immersion. The samples were immersed and left in water until they reached a constant weight indicating the full saturation (~7 days). The surface porosities were evaluated through the equilibrium magnetization data acquired from the untreated as well treated surfaces. Lastly, the gravimetric ratios were determined according to the following equation:

$$G = \frac{(m_S - m_0)}{m_0} \times 100 \quad (3)$$

where m_0 and m_S are the stone masses, in dry and water-saturated conditions.

2.6. Microscopic analysis of coating distribution

Micro-FTIR and SEM-EDS techniques were used for the analysis of the surface and the determination of the coating penetration depth.

By micro-FTIR analysis, the distribution of the acrylic polymers HR2 and HR3, even on rough and inhomogeneous substrates [45], was monitored by using the Nicolet iN10 Infrared Microscope (Thermo Fisher Scientific) equipped with spatial motorized stage (in the x, y and z directions) of 70 × 127 mm^2. The micro-FTIR equipment is provided with IR source cooled with air, a KBr beam splitter and the acquisitions were performed using Cassegrain IR/VIS objective, always aligned at 15X/0.7 FWD 16 mm, with an MCT-A detector cooled with liquid nitrogen. FTIR spectra were acquired in external reflection mode in the IR spectral region comprised between 4000 cm^{-1} and 675 cm^{-1} with a resolution of 8 cm^{-1} and 128 scans to increase the signal to noise ratio. All maps were composed by 100 spectra, organized in a 10 × 10 grid, each of which was acquired over an area of 100 × 100 μm^2. OMNIC Picta software was used to extrapolate the correlation maps for the reference, HR2-and HR3-coated samples by applying a first order correlation function in the region comprised between 1800 cm^{-1} and 1700 cm^{-1}; in fact, in this spectral region falls the characteristic absorption band of the carbonyl group of the acrylic polymers (at about 1750 cm^{-1}). The maximum value of correlation, equal to unity, was than assigned to the spectrum of the surface map, among all those acquired, which showed the highest intensity of the peak centered at 1750 cm^{-1}.

SEM-EDS technique was used to examine the surface topography and composition of the samples treated with silane-based products. Zeiss GeminiSEM 500 equipped with EDS OXFORD Aztec Energy with INCA X-ACT detector was used with a working distance of 9.0 mm and an accelerating voltage of 20 KeV. EDS microanalyses of reference and coated samples were acquired over an area of 1 mm^2 as a single map.

Subsequently, all the treated samples were cut to evaluate the penetration of the products inside the substrates. Therefore, an incision was made with a saw on the untreated face of all the specimens and then they were divided in two parts using hammer and chisel, thus avoiding artificial alteration of the composition due to cutting. In order to rationalize the tests related to the penetration of the protective coatings into the samples, micro-FTIR and SEM-EDS results were spatially correlated to the observations acquired by using an AxioZoom V16 (Zeiss)

stereomicroscope equipped with the Zen Blue 3.3 software.

3. Results and discussion

3.1. Coating dry residue, static contact angle and colorimetric parameters

All the protectives were applied "wet on wet" until saturation and the amount of the dry product was determined. In addition, the effect of the protectives on the stone surface properties was evaluated by measuring the static contact angle. Table 1 shows the mean dry weight values of the untreated Lecce stone samples, the mass of applied polymeric solution, the dry residue of polymer within the specimen volume, Q, determined by Eq. (1), and static contact angle.

In Table 1, when the coatings are compared to each other, strong differences are found out in terms of amount of polymer dry residues, which range from 0.28‰ to 14‰.

Acrylic polymers HR2 and HR3, whose aqueous dispersions contain the same concentration of product, show very similar values of dry protective deposited, comprised between 0.7 and 0.9‰. On the contrary, among silane-based coating, NP-coated samples show the lower Q value, while HY and WR are the products with the higher dry residues. These differences in the amount of polymer deposited may be due to the different concentration of silane precursors, not reported by the suppliers.

A comparison of our results with previously published data is not trivial, since the coating uptake, as well as the class of the protective agent, depends on the type of stone, *i.e.*, on its porosity and composition, and on the type of application. In fact, in a recent study, the amount of product applied on marble was approximately thirty times lower with respect to Lecce stone samples, due to its greater compactness which limited its penetration [46]. The method of application is also crucial as reported by Adamopoulos et al. [47] for marble samples. In fact, the product uptake was very different when it was deposited on the specimens by brush, spray or dip coating.

For what concerns the macroscopic effect of a hydrophobic coating, the contact angle of water with the sample surface (CA) is the more classical evaluation method. Due to the fast absorption of the water droplet, CA of the untreated reference samples could not be measured. Although the strong differences between the coating dry residues, CA values result very similar and, regardless of the nature of the applied polymer, they range around 135°, indicating a good hydrophobicity of all the coated surfaces.

Another important aspect of the protection treatment is the changes in colorimetric properties induced by the protective on the surface of the substrates; in fact, during the restoration interventions, particular attention has to be addressed towards the color alteration of the coated surfaces with respect to the original chromaticity of the materials.

The colorimetric coordinates of all samples of Lecce stone before the treatment were acquired and averaged to obtain the reference values of L*, a*, b* and E* that corresponded to 76.4 ± 1.3, 4.4 ± 0.5, 13.3 ± 1.0 and 77.7 ± 1.5, respectively. Mean colorimetric variation values and standard deviations of samples treated with all protective coatings are listed in Table 2.

According to the literature, color differences between coated and uncoated samples below 3 are not significant, being imperceptible to the human eye, while the accepted level for conservative purposes is a ΔE* <5 [48–50].

Samples treated with acrylic polymers, HR2 and HR3, appear slightly darker and yellower than the reference and the color differences of the specimens are not much higher than the perception limit and well below the accepted level for conservation purposes.

Regarding the siloxane polymers, HY produces a considerable and visible effect on the stone surface, being the ΔE* value of 8.0. In particular, analyzing the individual colorimetric coordinates, the treated surface of HY-coated specimens appears noticeably darker and yellower than the reference. The other silane-based coatings are almost entirely ineffective on the three chromatic coordinates, keeping the color of the support practically unchanged with a chromatic variation lower than the perception limit of the human eye.

3.2. Hygroscopic properties

One of the most important roles of protective coatings is to slow down the water absorption of the material from the environment, avoiding however to modify the porous characteristics of the material itself. The effect of the protective coatings was evaluated by performing the water uptake for capillarity of the reference specimens and of all the coated samples through their treated surfaces. The mean water absorption kinetics are reported in Fig. 1, while the raw data, *i.e.*, the kinetics of the three selected specimens for each coating, are shown Fig. S1.

The reference LS specimen rapidly absorbs water showing two hydration phases: one, faster, during the first hour of water uptake and the second, slower, recorded up to one week. The treated samples show a significantly different behavior from the reference one. In general, along the observation period, they are characterized by a complete hindrance of the water uptake for the first few hours, then by a single and more or less slow phase of hydration. The acrylic polymers, HR2 and HR3, induce a similar slowdown of the water absorption kinetics, however reaching an equilibrium water content similar to that of the reference.

On the contrary, among silane-based polymers, HY and WR completely hinder water absorption during capillary uptake as highlighted by an almost constant value of magnetization, M_{eq} ~5. About samples treated with NP, over time, they absorb water very slowly and, after one week of absorption their mean magnetization was 2.5 times lower than that of the reference. However, unlike the other coatings, the three samples treated with NP product (S Fig. S1c–e) show hydration behaviors with quite different slopes, as also highlighted in Fig. 1 by the large error bars associated with this set of samples.

The variabilities observed between the coated samples during water uptake are not perceived by the static CA measurements for which all the protectives are similar to each other. In fact, the measures of CA depend exclusively by the presence of the product on the substrate surface, while the NMR evidences are related to the distribution of the polymers within the specimen, which for our coatings is very different, as revealed by the microscopic observation reported in Section 3.4.

Table 1
For each coating, mean values of dry weight of the untreated samples, mass of added protective solution, dry residue of the product and static contact angle.

	Dry weight of untreated samples, g	Mass of protective solution, g	Q, ‰	Static contact angle, °
HR2	86.1 ± 2.1	1.6 ± 0.3	0.7 ± 0.4	136 ± 7
HR3	85.9 ± 1.4	1.7 ± 0.3	0.90 ± 0.04	135 ± 7
NP	85.3 ± 1.3	1.6 ± 0.3	0.28 ± 0.08	130 ± 5
HY	86.8 ± 2.8	3.4 ± 0.9	14 ± 8	141 ± 8
WR	83.2 ± 3.2	1.8 ± 0.2	11 ± 2	138 ± 9

Table 2
For each coating, mean values of colorimetric coordinates variations of the treated surface with respect to the reference one.

Sample	ΔL*	Δa*	Δb*	ΔE*
HR2	−1.9 ± 1.3	0.8 ± 0.7	2.3 ± 1.3	3.1 ± 1.4
HR3	−2.5 ± 0.8	0.9 ± 0.4	2.3 ± 0.9	3.5 ± 1.5
NP	0.0 ± 1.3	−0.1 ± 0.7	0.8 ± 0.9	0.8 ± 0.5
HY	−6.0 ± 1.3	1.8 ± 0.5	4.9 ± 1.9	8.0 ± 2.2
WR	−1.1 ± 1.3	0.3 ± 0.6	1.1 ± 1.0	1.6 ± 0.7

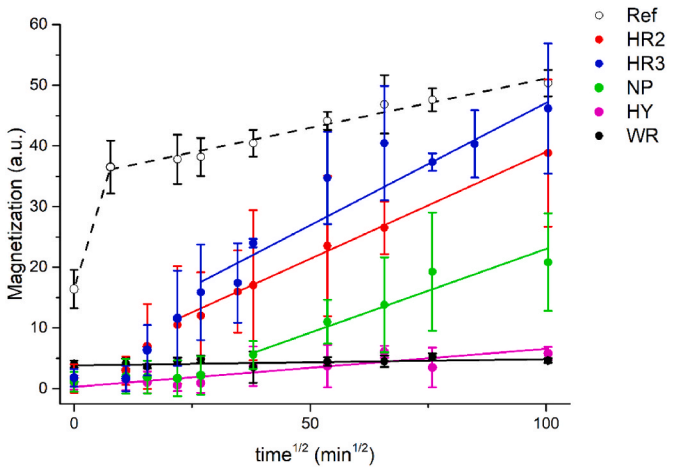

Fig. 1. For each coating, mean kinetics behavior of water absorptions by capillarity through the treated surface of the sample. For comparison, in dashed black line, the mean kinetics through one face of the reference sample.

3.3. Porosity

To understand if the effects induced by the protectives were due to an increased hydrophobicity of the treated surface or to a change of the stone porosity, the reference samples and all the treated ones were water saturated by immersion and analyzed through NMR porosimetry.

The measurements of T_2 distributions were performed on untreated and treated surfaces of all water saturated samples. At the same time, their gravimetric ratios were also evaluated. Useful information can be obtained by comparing water content NMR data and gravimetric ratios as reported in Table 3, by recalling that gravimetric measurements provide details on the average behavior of the whole sample, while NMR analysis shows highly meaningful surface information.

Gravimetric and magnetization data do not highlight significant differences between the samples treated with the acrylic protectives and the reference one. On the contrary, considering the silane-coated specimens, some evidence is noteworthy. NP-coated sample, when compared with the reference, shows the same mean value of gravimetric ratio, but a slight decrease in the magnetization value if the NMR measurements are performed on the treated surface. Such evidence can be ascribed to a partial occlusion of the porosity only in the immediate vicinity of the NP-treated surface. The porous structure of HY- and WR-coated samples result drastically affected by the coating, being their gravimetric data reduced by about 30% compared to the reference. The magnetization values of the treated surfaces are in complete accordance with the gravimetric result; in fact, they decrease, with the respect to the reference, by about 75% and 50%, respectively. Differently, the magnetization value of the untreated surface of HY-coated sample is reduced by about 30%, suggesting that the coating penetrates deeply throughout the stone, while that of WR-coated specimen is quite similar to the reference.

Table 3
For each coating, values of gravimetric ratio and magnetization data of treated (M_{TS}) and untreated (M_{US}) surfaces of the water saturated samples by immersion. The errors on all data are estimated around 5%.

	Gr, %	M_{TS}, (a.u.)	M_{US}, (a.u.)
REF	18	—	49[a]
HR2	18	52	50
HR3	18	50	52
NP	18	45	51
HY	12	12	35
WR	13	25	51

[a] Mean data of both 5 × 5 cm^2 surfaces of untreated reference samples.

It must be mentioned that during the immersion time of the WR-treated sample, part of the siloxane polymer comes out from the specimen making surfaces slimy, highlighting a partial dislocation in water of the coating polymer. This evidence was confirmed by ATR-FTIR spectrum of the *quasi*-dried spilled material, which shows the characteristic peak of the polymer at approximately 1070 cm^{-1} (Fig. S2). Anyway, WR technical data sheet reports that the product could not be applied under counterthrust of water. For a further check, the same WR-coated sample was re-dried and subjected to a new water uptake for capillarity. In Fig. S3 the results show a behavior similar to that of the reference stone, demonstrating the loss of a large amount of the polymer.

3.4. Microanalysis of treated surface and deep dispersion of coating into stone volume

Analysis of the treated surface of the samples as well as of their sections allowed to rationalize the results described so far. In fact, micro-FTIR and SEM-EDS investigations were performed to understand the homogeneity of the protective coating on the stone surface and, by correlating them with the stereomicroscopic observations, the diffusion of the protective into the specimens [45]. For this purpose, the choice between the two selected techniques was accomplished according to the nature of the polymer applied. On the one hand, samples coated with acrylic coatings, HR2 and HR3, were analyzed using micro-FTIR due to the presence of the strong stretching band of carbonyl groups of the polymers, as highlighted by the spectra of reference and HR2-treated sample reported in Fig. S4. On the other hand, silane-coated samples were studied using the SEM-EDS microanalysis focusing on silicon due to the low content of this element in the reference sample.

3.4.1. Acrylic coatings

Fig. 2 shows the correlation maps resulting from the micro-FTIR analysis of the reference (a) and acrylic-coated samples: HR2 (b) and HR3 (c).

The correlation factor (CF), ranging from 0.0 (full anticorrelation) to 1.0 (full correlation), is related to the presence of the stretching band of carbonyl groups along the surface and it is reported according to the map color bar. The image of the reference sample (Fig. 2a) is fully homogeneous and its intensity corresponds to the middle of the map color bar with CF = 0.5, which means no correlation. Differently, high correlation colormaps (CF > 0.9) are obtained for specimens covered with the acrylic polymers indicating that the coatings are homogeneously dispersed on the treated surface, except for some small green areas.

To understand the degree of penetration of these coatings inside the stone material, the correlative analysis between stereomicroscope images and micro-FTIR data was carried out along the 2 cm section of the cut samples; the results are reported in Fig. 3. As described in the Experimental section, samples were broken, rather than cut with a saw, to avoid the dislocation of the protective.

The images clearly show that HR2 (Fig. 3a) penetrates deeper inside the stone samples than the HR3 polymer (Fig. 3b); in particular, HR2 reaches the correlation value of the reference at about 2.3 mm from the surface, but its presence is identified also in the middle of the sample at about 12 mm of depth. On the contrary, HR3 diffuses only up to 1 mm from the treated surface.

3.4.2. Silane-based coatings

Fig. 4 shows the SEM images of reference and silane-coated samples, where the distribution of silicon, determined by EDS microanalysis, is evidenced in red.

The EDS microanalysis of the reference sample (Fig. 4a) shows some red spots associated with the presence of silicon portions that could be due to inclusion of silicates into the carbonate matrix of Lecce stone.

SEM-EDS images of the treated surfaces show, over the typical silicon spots of the reference, a uniform red patina due to the ubiquitous

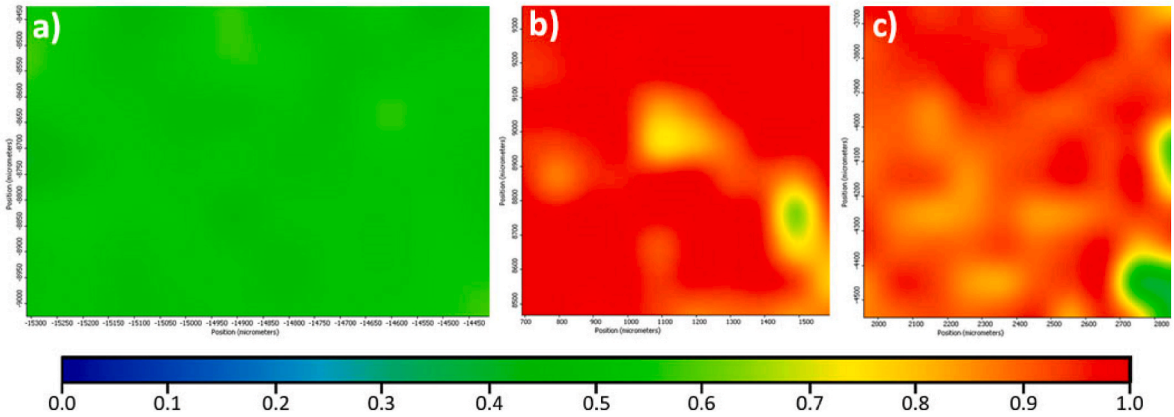

Fig. 2. Correlation map of reference (a), HR2-coated (b) and HR3-coated (c) samples.

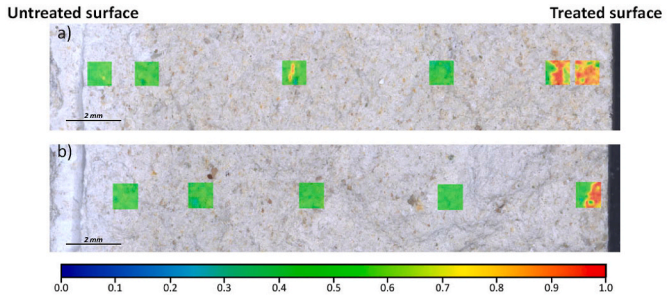

Fig. 3. Stereomicroscope images correlated with micro-FTIR analysis of the samples treated with acrylic polymers HR2 (a) and HR3 (b).

presence of silicon. In particular, for NP-coated sample (Fig. 4b) a drastic change in morphology was observed, as highlighted by the formation of plaques of siloxane polymer on the stone surface. On the contrary, HY- and WR-coated samples (Fig. 4c and d) appears very similar to the reference in terms of morphology, but with a slight red coloration over all the investigated areas, indicating a widespread increase in silicon content.

Even with silane-based polymers, the degree of penetration of the coating, along the 2 cm section of the cut sample, was studied by correlating stereomicroscope images and SEM-EDS analysis. The results are reported in Fig. 5.

All the investigated samples show the previously described red patina independently of the distance from the treated surface, clearly indicating the presence of silane-based polymers up to the untreated face, much more evident for the HY- and WR-coated specimens than for the NP-coated one.

To deal with the distribution of the protectives in the stone specimens, it was needed a more quantitative approach for analyzing the SEM-EDS images.

As for silicon, also low content of aluminum was detected on the reference sample, due to the presence of aluminum-silicate inclusions in

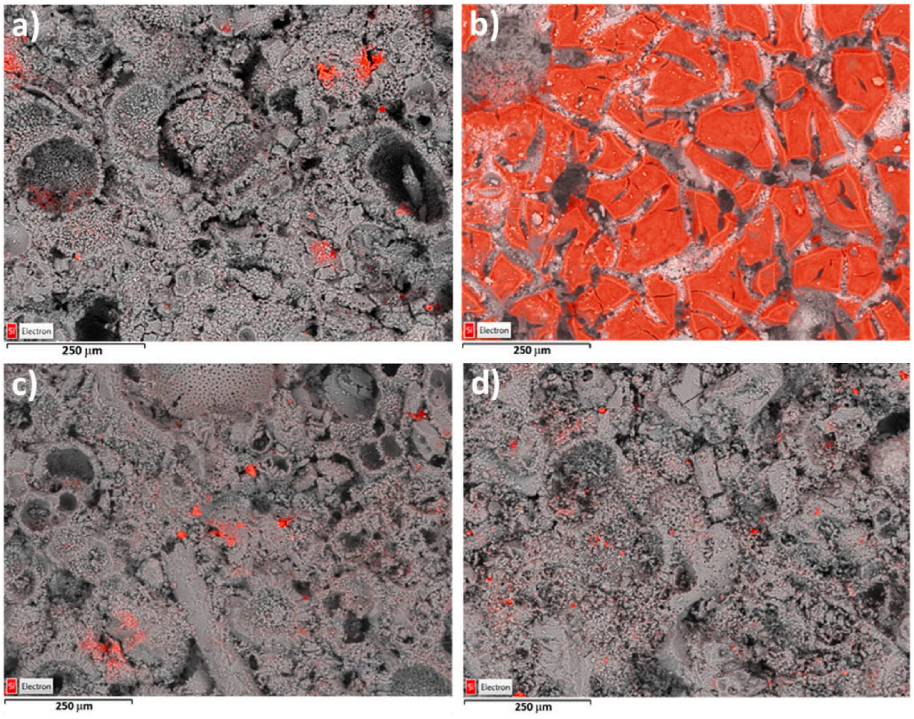

Fig. 4. SEM-EDS images of the reference (a) and of the samples coated with NP (b), HY (c), and WR (d). The presence of silicon, highlighted by EDS, is evidenced in red. (For interpretation of the references to color in this figure legend, the reader is referred to the Web version of this article.)

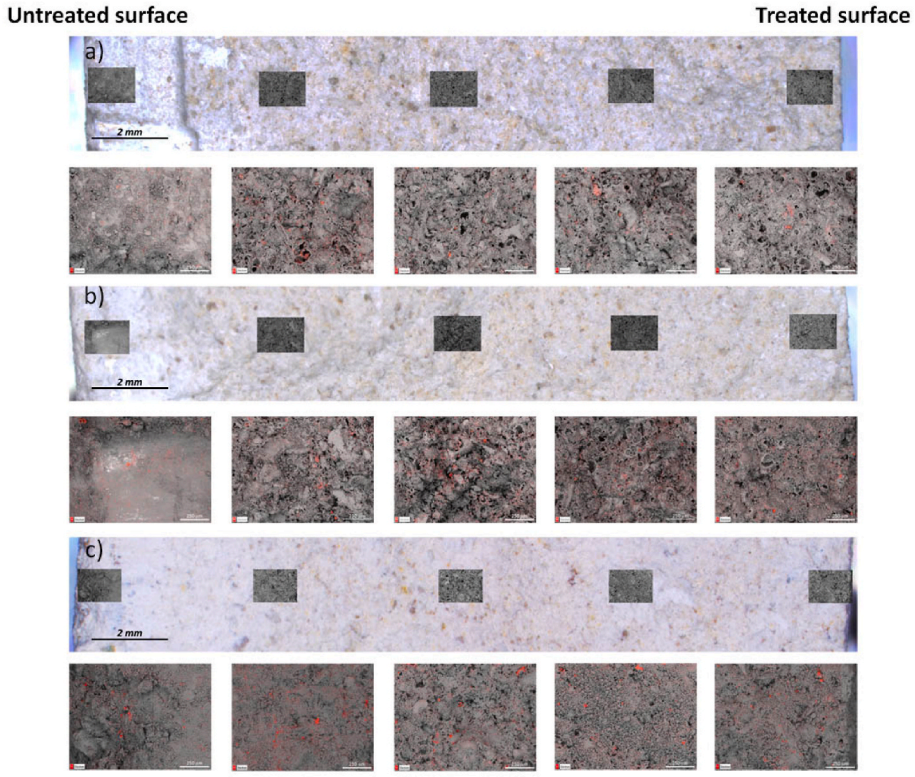

Fig. 5. Stereomicroscope images correlated with SEM-EDS microanalysis of specimens coated with silane-based polymers, NP (a), HY (b) and WR (c).

the lithotype. In fact, by assigning the yellow color to alluminum on the SEM images, the red spots ascribed to silicon became orange as shown in Fig. S5. The Si/Al ratio determined on six different areas of the reference stone surface resulted to be always about 2.0. Then, this ratio was set as a threshold value to discriminate intrinsic silicon from that added with silane-based polymers.

3.5. Comparison between the effect of acrylic and silane-based coatings

The means of the correlation factors of the micro-FTIR color maps (Fig. 2) and of Si/Al ratios evaluated from SEM-EDS (Fig. 4), concerning the reference and the treated surfaces for each coating, are reported in Table 4.

Compared to the reference, the acrylic coatings appear very similar, with mean correlation factors higher than 0.9. This similarity between the acrylic polymers is also found out by looking at the dry product residues that range around 0.8‰ for both protectives (Table 1). For the silane-treated samples, significantly different evidence is observed for Si/Al ratios as well as for the amount of the polymer dry residues (Table 1). The NP-coated samples, with the highest mean value of the Si/Al ratio (equal to 70), have the least quantity of dry residue (0.3‰), while the HY- and WR-treated samples show Si/Al values of only 3.5 and 2 times higher than that of the reference, despite the higher values of dry polymer residues, being respectively 14 and 11‰.

These evidences suggested that, while NP mainly remained on the stone surface, both HY and WR penetrated along the section of the samples.

The coating penetration into the sample was evaluated plotting the mean correlation factors for acrylic polymers (Fig. 6a), and the Si/Al ratios for silane-based ones (Fig. 6b) along the sample depths just visualized respectively in Figs. 3 and 5.

It is evident from Fig. 6a that HR2 penetrated deeper up to half section of the sample, while the degree of penetration of HR3 rapidly decayed to the reference correlation factor within the first 5 mm from the treated surface. The large error bars found for some points refer to those areas where the acrylic polymers and the constituent material coexist (Fig. 3).

Fig. 6b confirms the previously formulated hypothesis about the silane coatings; in fact, NP polymer remained almost completely on the treated surface and its content along the sample depth decreased rapidly towards a value slightly higher than the threshold one. Instead, HY and WR resulted more distributed from the treated to the untreated surfaces. Moreover, comparing the effect of these two polymers, significant amount of HY penetrates up to 5 mm from the treated surface, while the WR polymer diffuses more homogeneously from the treated surface to the untreated one. Despite the relative low surface amount of HY and WR, respect to NP, their persistence until the respective untreated surfaces are demonstrated by Si/Al ratios, that result double when compared with that of reference.

The microscopic observations combined with micro-FTIR and SEM-EDS analyses were in complete accordance with the results obtained with the just discussed macroscopic characterization that allowed to discriminate the protectives according to their hygroscopic and porosity properties. In fact, the samples treated with the HR2 acrylic polymer, compared to the HR3-coated samples, showed a lower rate of water absorption by capillarity and a greater penetration of the coating inside the stone material. In both acrylic-coated samples, especially at short times of water absorption, the kinetics were very slow, demonstrating a relevant surface hydrophobicity of the treated samples. However, with nearly the same amounts of residual dry product, the acrylic-coated

Table 4
For reference and coated samples, (on the left) mean correlation factors of surfaces treated with acrylic HR2 and HR3 polymers; (on the left) mean value of Si/Al ratios for surfaces treated with silane-based NP, HY, and WR polymers.

Correlation factor			Si/Al ratio			
REF	HR2	HR3	REF	NP	HY	WR
0.52 ± 0.04	0.97 ± 0.05	0.91 ± 0.09	1.9 ± 0.2	70 ± 7	7.0 ± 0.9	4.0 ± 0.7

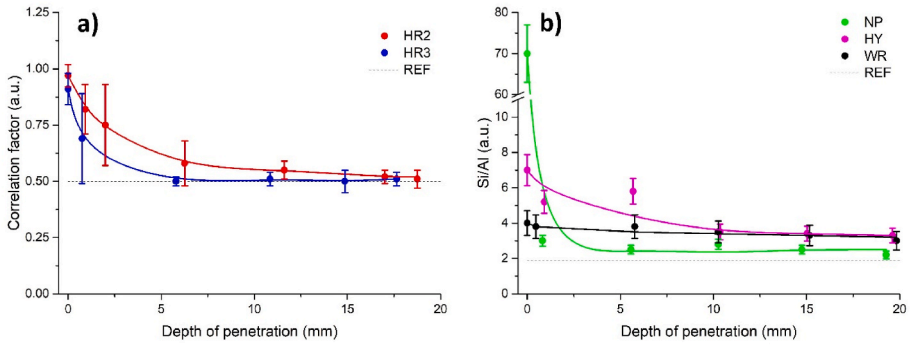

Fig. 6. For each coating, penetration depth into the stone, expressed as mean value of the correlation factor (a), or of the Si/Al ratio (b). In each panel, the black dotted line corresponds to the threshold value of the reference.

samples, when water saturated by immersion, showed similar gravimetric and NMR porosity data with respect to the reference samples, then revealing an open porosity equal to that of an untreated Lecce stone.

Among the silane-coated samples, NP-coated ones showed an out of range fraction of polymer on the stone surface, in the form of more or less large plaques. According to the compactness of these plaques, water could be absorbed with different timing, thus explaining the high variability of the water uptake rates of the three samples treated with this polymer (see Fig. S1c). The water-repellent behavior of NP-coated samples mainly depends on the random morphology of polymer plaques, as also confirmed by the NMR porosimetry.

The other two silane-based polymers, HY and WR, according to microanalysis evidence, were ubiquitously distributed on the surface and on the entire volume stone, clearly highlighting a higher degree of penetration than that of the other products. This behavior, along with the higher amounts of dry residues, could explain the almost total occlusion effects observed during the entire capillary water uptake and under water-saturated conditions. For HY-coated sample, the low gravimetric factor as well as both magnetization values shown in Table 3 confirm this analysis. On the contrary, the porosity on both the faces of WR-coated sample does not seem to show the same behavior, probably due to the loss of polymer when the sample was subjected to water immersion.

4. Conclusions

This paper reports the comparison between commercially available silane-based products and two newly synthesized acrylic ones, when they are used as water-repellent protective agents to prevent the deterioration of limestone. The macroscopic and microscopic investigations allowed to correlate the hygroscopic behavior of the treated stone with the distribution of the product on the stone surface and its penetration depth into the specimens. The results highlight that the two silane products, HY and WR, completely hindered the water absorption, spread from the treated to the untreated surface, occluding the pores of the stone. On the contrary, the two acrylic coatings, HR2 and HR3, and the silane-based NP product were mainly distributed on the stone surface, slowing down the water-uptake but still reaching, at very long time, an equilibrium water content similar to that of the reference. Although there is not yet a standardized protocol to detect any kind of interference between protective product and stone material, in addition to contact angle, colorimetry and gravimetry, widely used for this purpose, here we used NMR relaxometry to test the hygroscopic properties and porous structure of the stone before and after the treatment. Furthermore, powerful analyses were performed, through micro-FTIR and SEM-EDS techniques, to go into details on the microscopic distribution of the coating on the surface and into the volume of the sample.

It is beyond doubts that this kind of data could be useful to choose the most suitable product according to the artwork to be protected and the environment in which it is placed.

Funding

This work was supported by the Italian Ministry of Education, Universities and Research (MIUR): project Smart Cities and Communities and Social Innovation on Cultural Heritage (SCN_00520).

CRediT authorship contribution statement

Francesco Gabriele: Investigation, Data curation, Visualization, Writing – original draft, Writing – review & editing. **Cinzia Casieri:** Conceptualization, Writing – review & editing, Funding acquisition, Supervision. **Alice Vetrano:** Investigation, Data curation, Writing – original draft. **Nicoletta Spreti:** Conceptualization, Writing – review & editing, Funding acquisition, Supervision.

Declaration of competing interest

The authors declare that they have no known competing financial interests or personal relationships that could have appeared to influence the work reported in this paper.

Data availability

Data will be made available on request.

Acknowledgment

The authors thank Chiara Gandolfi (Icap Leather Chem SpA) for supplying the acrylic products. The also would like to acknowledge Dr. Maria Giammatteo, Dr. Lorenzo Arrizza and Dr. Angelo Sarra (Microscopy Centre, University of L'Aquila) for the stereomicroscope, SEM-EDS and micro-FTIR analyses.

Appendix A. Supplementary data

Supplementary data to this article can be found online at https://doi.org/10.1016/j.matchemphys.2023.128194.

References

[1] E. Doehne, C.A. Price, Stone Conservation: an Overview of Current Research, second ed., Getty Publications, Los Angeles, 2010.
[2] P. Brimblecombe, Environment and architectural stone, in: S. Siegesmund, R. Snethlage (Eds.), Stone in Architecture: Properties, Durability, fifth ed., Springer-Verlag Berlin Heidelberg, 2014, pp. 317–347, https://doi.org/10.1007/978-3-642-45155-3_5.
[3] T. Warscheid, J. Braams, Biodeterioration of stone: a review, Int. Biodeterior. Biodegrad. 46 (2000) 343–368, https://doi.org/10.1016/S0964-8305(00)00109-8.

[4] Y. Nuhoglu, E. Oguz, H. Uslu, A. Ozbek, B. Ipekoglu, I. Ocak, I. Hasenekoglu, The accelerating effects of the microorganisms on biodeterioration of stone monuments under air pollution and continental-cold climatic conditions in Erzurum, Turkey, Sci. Total Environ. 364 (2006) 272–283, https://doi.org/10.1016/j.scitotenv.2005.06.034.
[5] E. Stanaszek-Tomal, Environmental factors causing the development of microorganisms on the surfaces of national cultural monuments made of mineral building materials - review, Coatings 10 (2020) 1203, https://doi.org/10.3390/coatings10121203.
[6] F. Gherardi, Current and future trends in protective treatments for stone heritage, in: F. Gherardi, P.-N. Maravelaki (Eds.), Conserving Stone Heritage. Cultural Heritage Science, Springer, Cham, Switzerland, 2022, pp. 137–176, https://doi.org/10.1007/978-3-030-82942-1_5.
[7] A.E. Charola, Water-repellent treatments for building stones: a practical overview, APT Bull. 26 (1995) 10–17, https://doi.org/10.2307/1504480.
[8] UNI EN 16581, Conservation of Cultural Heritage - Surface Protection for Porous Inorganic Materials - Laboratory Test Methods for the Evaluation of the Performance of Water Repellent Products, 2014.
[9] A. Sierra-Fernandez, L.S. Gomez-Villalba, M.E. Rabanal, R. Fort, New nanomaterials for applications in conservation and restoration of stony materials: a review, Mater. Construcción 67 (2017) e107, https://doi.org/10.3989/mc.2017.07616.
[10] M. Frigione, M. Lettieri, Novel attribute of organic-inorganic hybrid coatings for protection and preservation of materials (stone and wood) belonging to cultural heritage, Coatings 8 (2018) 319, https://doi.org/10.3390/coatings8090319.
[11] A. Ershad-Langroudi, H. Fadaei, K. Ahmadi, Application of polymer coatings and nanoparticles in consolidation and hydrophobic treatment of stone monuments, Iran. Polym. J. (Engl. Ed.) 28 (2019) 1–19, https://doi.org/10.1007/s13726-018-0673-y.
[12] S.A. Ruffolo, M.F. La Russa, Nanostructured coatings for stone protection: an overview, Front. Mater. 6 (2019) 147, https://doi.org/10.3389/fmats.2019.00147.
[13] A. Artesani, F. Di Turo, M. Zucchelli, A. Traviglia, Recent advances in protective coatings for cultural heritage-an overview, Coatings 10 (2020) 217, https://doi.org/10.3390/coatings10030217.
[14] Y. Cao, A. Salvini, M. Camaiti, Current status and future prospects of applying bioinspired superhydrophobic materials for conservation of stone artworks, Coatings 10 (2020) 353, https://doi.org/10.3390/coatings10040353.
[15] F. Cappitelli, F. Villa, P. Sanmartín, Interactions of microorganisms and synthetic polymers in cultural heritage conservation, Int. Biodeterior. Biodegrad. 163 (2021), 105282, https://doi.org/10.1016/j.ibiod.2021.105282.
[16] I. Karapanagiotis, P.N. Manoudis, Superhydrophobic and superamphiphobic materials for the conservation of natural stone: an overview, Construct. Build. Mater. 320 (2022), 126175, https://doi.org/10.1016/j.conbuildmat.2021.126175.
[17] M.L. Tabasso, Acrylic polymers for the conservation of stone: advantages and drawbacks, APT Bull. 26 (1995) 17–21, https://doi.org/10.2307/1504445.
[18] E. Carretti, L. Dei, Physicochemical characterization of acrylic polymeric resins coating porous materials of artistic interest, Prog. Org. Coating 49 (2004) 282–289, https://doi.org/10.1016/j.porgcoat.2003.10.011.
[19] M. Favaro, R. Mendichi, F. Ossola, U. Russo, S. Simon, P. Tomasin, P.A. Vigato, Evaluation of polymers for conservation treatments of outdoor exposed stone monuments. Part I: photo-oxidative weathering, Polym. Degrad. Stabil. 91 (2006) 3083–3096, https://doi.org/10.1016/j.polymdegradstab.2006.08.012.
[20] G. Alessandrini, M. Aglietto, V. Castelvetro, F. Ciardelli, R. Peruzzi, L. Toniolo, Comparative evaluation of fluorinated and unfluorinated acrylic copolymers as water-repellent coating materials for stone, J. Appl. Polym. Sci. 76 (2000) 962–977, https://doi.org/10.1002/(SICI)1097-4628(20000509)76:6<962::AID-APP24>3.0.CO;2-Z.
[21] T. Poli, L. Toniolo, Protection efficacy of fluorinated acrylic copolymers applied on historical Italian marbles, MRS Online Proc. Libr. 852 (2005) 288–294, https://doi.org/10.1557/PROC-852-OO6.3.
[22] V. Sabatini, H. Farina, A. Montarsolo, E. Pargoletti, M.A. Ortenzi, G. Cappelletti, Fluorinated polyacrylic resins for the protection of cultural heritages: the effect of fluorine on hydrophobic properties and photochemical stability, Chem. Lett. 47 (2018) 280–283, https://doi.org/10.1246/cl.171020.
[23] V. Sabatini, C. Cattò, G. Cappelletti, F. Cappitelli, S. Antenucci, H. Farina, M. A. Ortenzi, S. Camazzola, G. Di Silvestro, Protective features, durability and biodegration study of acrylic and methacrylic fluorinated polymer coatings for marble protection, Prog. Org. Coating 114 (2018) 47–57, https://doi.org/10.1016/j.porgcoat.2017.10.003.
[24] F. Sbardella, L. Pronti, M.L. Santarelli, J.M.A. Gonzàlez, M.P. Bracciale, Waterborne acrylate-based hybrid coatings with enhanced resistance properties on stone surfaces, Coatings 8 (2018), 105897, https://doi.org/10.3390/coatings8080283.
[25] F. Sbardella, M.P. Bracciale, M.L. Santarelli, J.M. Asua, Waterborne modified-silica/acrylates hybrid nanocomposites as surface protective coatings for stone monuments, Prog. Org. Coating 149 (2020) 283, https://doi.org/10.1016/j.porgcoat.2020.105897.
[26] L. Li, B. Li, J. Dong, J. Zhang, Roles of silanes and silicones in forming superhydrophobic and superoleophobic materials, J. Mater. Chem. 4 (2016) 13677–13725, https://doi.org/10.1039/c6ta05441b.
[27] E. Tesser, F. Antonelli, L. Sperni, R. Ganzerla, N.-P. Maravelaki, Study of the stability of siloxane stone strengthening agents, Polym. Degrad. Stabil. 110 (2014) 232–240, https://doi.org/10.1016/j.polymdegradstab.2014.08.022.
[28] B. Sacchi, S. Vettori, A. Andreotti, L. Rampazzi, M.P. Colombini, P. Tiano, Assessment of water repellent treatments for the stone of the Matera Cathedral facade (Italy), Int. J. Architect. Herit. 16 (2022) 365–373, https://doi.org/10.1080/15583058.2020.1782532.
[29] M. Lettieri, M. Masieri, Performances and coating morphology of a siloxane-based hydrophobic product applied in different concentrations on a highly porous stone, Coatings 6 (2016) 60, https://doi.org/10.3390/coatings6040060.
[30] M. Tortora, M. Chiarini, N. Spreti, C. Casieri, 1H-NMR-relaxation and colorimetry for evaluating nanopolymeric dispersions as stone protective coatings, J. Cult. Herit. 44 (2020) 204–210, https://doi.org/10.1016/j.culher.2019.12.014.
[31] M. Hosseini, I. Karapanagiotis, Advanced Materials for the Conservation of Stone, first ed., Springer, Cham, 2018 https://doi.org/10.1007/978-3-319-72260-3.
[32] G. Wheeler, Alkoxysilanes and the Consolidation of Stone, Getty Publications, Los Angeles, 2005.
[33] V. Bortolotti, M. Camaiti, C. Casieri, F. De Luca, P. Fantazzini, C. Terenzi, Water absorption kinetics in different wettability conditions studied at pore and sample scales in porous media by NMR with portable single-sided and laboratory imaging devices, J. Magn. Reson. 181 (2006) 287–295, https://doi.org/10.1016/j.jmr.2006.05.016.
[34] C. Casieri, C. Terenzi, F. De Luca, Noninvasive monitoring of moisture uptake in Ca$(NO_3)_2$-polluted calcareous stones by 1H-NMR relaxometry, Magn. Reson. Chem. 53 (2015) 15–21, https://doi.org/10.1002/mrc.4173.
[35] V. Di Tullio, N. Proietti, D. Capitani, I. Nicolini, A.M. Mecchi, NMR depth profiles as a non-invasive analytical tool to probe the penetration depth of hydrophobic treatments and inhomogeneities in treated porous stones, Anal. Bioanal. Chem. 400 (2011) 3151–3164, https://doi.org/10.1007/s00216-011-4968-5.
[36] V. Di Tullio, M. Cocca, R. Avolio, G. Gentile, N. Proietti, P. Ragni, M.E. Errico, D. Capitani, M. Avella, Unilateral NMR investigation of multifunctional treatments on stones based on colloidal inorganic and organic nanoparticles, Magn. Reson. Chem. 53 (2015) 64–77, https://doi.org/10.1002/mrc.4136.
[37] F. Rosi, L. Cartechini, D. Sali, C. Miliani, Recent trends in the application of fourier transform infrared (FT-IR) spectroscopy in heritage science: from micro- to non-invasive FT-IR, Phys. Sci. Rev. 4 (2019), 20180006, https://doi.org/10.1515/psr-2018-0006.
[38] E.J. Vermeij, P.D. Zoon, S.B.C.G. Chang, I. Keereweer, R. Pieterman, R.R. R. Gerretsen, Analysis of microtraces in invasive traumas using SEM/EDS, Forensic Sci. Int. 214 (2012) 96–104, https://doi.org/10.1016/j.forsciint.2011.07.025.
[39] S. Bugani, M. Camaiti, L. Morselli, E. Van De Casteele, K. Janssens, Investigation on porosity changes of Lecce stone due to conservation treatments by means of x-ray nano- and improved micro-computed tomography: preliminary results, X Ray Spectrom. 36 (2007) 316–320, https://doi.org/10.1002/xrs.976.
[40] S. Bugani, M. Camaiti, L. Morselli, E. Van De Casteele, K. Janssens, Investigating morphological changes in treated vs. untreated stone building materials by x-ray micro-CT, Anal. Bioanal. Chem. 391 (2008) 1343–1350, https://doi.org/10.1007/s00216-008-1946-7.
[41] A. Calia, M.L. Tabasso, A.M. Mecchi, G. Quarta, The study of stone for conservation purposes: Lecce stone (southern Italy), Geol. Soc. Spec. Publ. 391 (2014) 139–156, https://doi.org/10.1144/SP391.8.
[42] UNI EN 15886, Conservation of cultural property - test methods - colour measurement of surfaces, Official Italian version of EN 15886 (2010), 15886, 2010.
[43] UNI EN 15801, Conservation of Cultural Property - Test Methods - Determination of Water Absorption by Capillarity, 2010, 15801.
[44] C. Casieri, L. Senni, M. Romagnoli, U. Santamaria, F. De Luca, Determination of moisture fraction in wood by mobile NMR device, J. Magn. Reson. 171 (2004) 364–372, https://doi.org/10.1016/j.jmr.2004.09.014.
[45] F. Casadio, L. Toniolo, Polymer treatments for stone conservation: methods for evaluating penetration depth, J. Am. Inst. Conserv. 43 (2004) 3–21, https://doi.org/10.1179/019713604806112623.
[46] Y. Cao, A. Salvini, M. Camaiti, Oligoamide grafted with perfluoropolyether blocks: a potential protective coating for stone materials, Prog. Org. Coating 111 (2017) 164–174, https://doi.org/10.1016/j.porgcoat.2017.05.010.
[47] F.G. Adamopoulos, E.C. Vouvoudi, E. Pavlidou, D.S. Achilias, I. Karapanagiotis, TEOS-based superhydrophobic coating for the protection of stone-built cultural heritage, Coatings 11 (2021) 135, https://doi.org/10.3390/coatings11020135.
[48] D. Pinna, Can we do without biocides to cope with biofilms and lichens on stone heritage? Int. Biodeterior. Biodegrad. 172 (2022), 105437 https://doi.org/10.1016/j.ibiod.2022.105437.
[49] G. Vigliano, Graffiti and Antigraffiti Project, 2009. https://www.oocities.org/emuseoros/Docs/antigrafiti.htm. (Accessed 18 May 2023).
[50] A. Chatzigrigoriou, I. Karapanagiotis, I. Poulios, Superhydrophobic coatings based on siloxane resin and calcium hydroxide nanoparticles for marble protection, Coatings 10 (2020) 334, https://doi.org/10.3390/coatings10040334.